Surface-Dependent Transitions during Self-Assembly of Phospholipid Membranes on Mica, Silica, and Glass

Martin Beneš,[†] Didier Billy,[‡] Aleš Benda,[†] Han Speijer,[§] Martin Hof,[†] and Wim Th. Hermens*[,§]

J. Heyrovský Institute of Physical Chemistry, Academy of Sciences of the Czech Republic, Centre for Complex Molecular Systems and Biomolecules, Dolejškova 3, 18223 Prague, Czech Republic, Medtronic Bakken Research Center, Endepolsdomein 5, 6229 GW Maastricht, The Netherlands, and Cardiovascular Research Institute Maastricht, Maastricht University, P.O. Box 616, 6200 MD Maastricht, The Netherlands

Received May 13, 2004. In Final Form: August 30, 2004

Formation of supported membranes by exposure of solid surfaces to phospholipid vesicles is a much-used technique in membrane research. Freshly cleaved mica, because of its superior flatness, is a preferred support, and we used ellipsometry to study membrane formation kinetics on mica. Neutral dioleoylphosphatidylcholine (DOPC) and negatively charged dioleoyl-phosphatidylserine/dioleoyl-phosphatidylcholine (20% DOPS/80% DOPC) vesicles were prepared by sonication. Results were compared with membrane formation on silica and glass, and the influence of stirring, buffer, and calcium was assessed. Without calcium, DOPC vesicles had a low affinity ($K_d \approx 30\ \mu M$) for mica, and DOPS/DOPC vesicles hardly adsorbed. Addition of calcium promptly caused condensation of the adhering vesicles, with either loss of excess lipid or rapid additional lipid adsorption up to full surface coverage. Vesicle−mica interactions dominate the adsorption process, but vesicle−vesicle interactions also seem to be required for the condensation process. Membranes on mica proved unstable in Tris−HCl buffer. For glass, transport-limited adsorption of DOPC and DOPS/DOPC vesicles with immediate condensation into bilayers was observed, with and without calcium. For silica, vesicle adsorption was also rapid, even in the absence of calcium, but the transition to condensed layers required a critical surface coverage of about 50% of bilayer mass, indicating vesicle−vesicle interaction. For all three surfaces, additional adsorption of DOPC (but not DOPS/DOPC) vesicles to condensed membranes was observed. DOPC membranes on mica were rapidly degraded by phospholipase A2 (PLA2), which pleads against the role of membrane defects as initial PLA2 targets. During degradation, layer thickness remained unchanged while layer density decreased, in accordance with recent atomic force microscopy measurements of gel-phase phospholipid degradation by PLA2.

Introduction

Studies of phospholipid membranes and membrane−protein interactions often require deposition of the membrane on solid supports. This is true for classical methods such as electron diffraction but also for more recently introduced techniques for membrane study at (sub)-nanometer resolution, like surface plasmon resonance (SPR),[1] total internal reflection fluorescence (TIRF),[2] atomic force microscopy (AFM),[3] quartz crystal microbalance with dissipation monitoring (QCM-D),[4] and fluorescence correlation spectroscopy (FCS).[5]

The classical Langmuir−Blodgett stacking technique,[6] with each monolayer deposited separately, is sure to produce the phospholipid bilayers required for biological membrane models, but such membranes may contain defects[7] that may strongly influence bilayer−protein interactions.[8] In the 1970s, new supported membrane preparations were produced by controlled rehydration of phospholipids that were first dried on the supports.[9,10] Although easier than stacking, these techniques generally produced multilayer structures rather than bilayers.

It was an improvement when membranes were produced by exposure of supports to suspensions of unilamellar phospholipid vesicles.[11] Adsorption and fusion of such vesicles is more likely to produce bilayers, but the quoted study also showed that incorporated transmembrane T-cell receptors had no lateral mobility. More recently it was demonstrated that, depending on the support, phospholipids, and buffer composition, bilayers will often not be formed.[12−15]

Surface roughness may well influence membrane deposition, and (metal-sputtered) glass or silicon wafers may have irregularities of the order of bilayer thickness.[16,17] Even a roughness in the subnanometer range caused

* Corresponding author. Tel: +31-43-3881650. Fax: +31-43-3670916. E-mail: w.hermens@carim.unimaas.nl.
[†] Academy of Sciences of the Czech Republic.
[‡] Medtronic Bakken Research Center.
[§] Maastricht University.

(1) Salamon, Z.; Wang, Y.; Tollin, G.; Macleod, H. A. *Biochim. Biophys. Acta* **1994**, *1195*, 267−275.
(2) Axelrod, D.; Thompson, N. L.; Burghardt, T. P. *J. Microsc.* **1983**, *129*, 19−28.
(3) Reviakine, I.; Brisson, A. *Langmuir* **2000**, *16*, 1806−1815.
(4) Janshoff, A.; Galla, H.-J.; Steinem, C. *Angew. Chem., Int. Ed.* **2000**, *39*, 4004−4032.
(5) Benda, A.; Beneš, M.; Mareček, V.; Lhotský, A.; Hermens, W. Th.; Hof, M. *Langmuir* **2003**, *19*, 4120−4126.
(6) Blodgett, K. B. *J. Am. Chem. Soc.* **1935**, *57*, 1007−1022.
(7) Fischer, A.; Sackmann, E. *J. Phys.* **1984**, *45*, 517−527.
(8) Grandbois, M.; Clausen-Schumann, H.; Gaub, H. *Biophys. J.* **1998**, *74*, 2398−2404.
(9) Levine, Y. K.; Wilkins, M. H. *Nat. New Biol.* **1971**, *230*, 69−72.
(10) Badley, R. A.; Martin, W. G.; Schneider, H. *Biochemistry* **1973**, *12*, 268−275.
(11) Brian, A. A.; McConnell, H. M. *Proc. Natl. Acad. Sci. U.S.A.* **1984**, *81*, 6159−6163.
(12) Kalb, E.; Tamm, L. K. *Thin Solid Films* **1992**, *210/211*, 763−765.
(13) Nollert, P.; Kiefer, H.; Jähnig, F. *Biophys. J.* **1995**, *69*, 1447−1455.
(14) Keller, C. A.; Kasemo, B. *Biophys. J.* **1998**, *75*, 1397−1402.
(15) Reviakine, I.; Simon, A.; Brisson, A. *Langmuir* **2000**, *16*, 1473−1477.
(16) Rasigni, G.; Varnier, F.; Rasigni, M.; Palmari, J. P.; Llebaria, A. *Phys. Rev.* **1982**, *B15*, 2315−2323.
(17) Gauthier, S.; Aimé, J. P.; Bouhacina, T.; Attias, A. J.; Desbat, B. *Langmuir* **1996**, *12*, 5126−5137.

10.1021/la048811u CCC: $27.50
Published on Web 10/16/2004

disturbed annexin V crystallization on deposited bilayers.[18] Today, freshly cleaved mica is the only readily available surface with atomic scale flatness and this has made it a preferred substrate. It was shown recently that such mica surfaces also allow study of deposited membranes by ellipsometry and confocal FCS.[19]

In the present study, ellipsometry is used for the first time to study self-assembling phospholipid membranes on mica. This technique allows real-time monitoring of surface mass, thickness, and refractive index (density) of the membrane, and thereby of adsorption and transition kinetics. Results are compared to membrane formation on two other often-used surfaces, silica-covered silicon slides and glass. The influence of stirring, phospholipid charge, buffer composition, and presence of calcium was studied, as well as the breakdown of membranes on mica by phospholipase A2.

Materials and Methods

Proteins, Phospholipids, and Vesicle Preparation. Phospholipase A2 (PLA2) from snake venom (Naja moçambique) and bovine serum albumin (BSA) were obtained from Sigma (St. Louis, MO). Dioleoyl-phosphatidylcholine (DOPC) and dioleoyl-phosphatidylserine (DOPS) were from Avanti Polar Lipids (Alabaster, AL). Buffers with pH 7.4 were prepared with pure water (Milli-Q3 system, Millipore, Etten-Leur, The Netherlands) and contained either 10 mM Hepes with 150 mM NaCl or 50 mM Tris with 100 mM NaCl. They also contained 2 mM $CaCl_2$ or, for calcium-free experiments, 2 mM EDTA. The EDTA was added to remove traces of calcium from solutions, because irreproducible results were obtained with surfaces first treated with calcium and then exposed to calcium-free buffer without EDTA. All chemicals were of the highest grade available. To reduce ellipsometer scatter, buffers were passed through a 0.2 μm syringe filter (Schleicher & Schuell, Dassel, Germany). Refractive indexes of buffers were determined by refractometry (Abbe Refractometer 1T, Atago, Tokyo, Japan).

Either pure DOPC or a 20 mol % DOPS/80 mol % DOPC mixture (DOPS/DOPC) was used. Small unilamellar vesicles of about 25 nm average diameter[20] were prepared from lipids in chloroform, dried under nitrogen. The dry films were resuspended in buffer, and the turbid suspensions, cooled by water, were sonicated to clarity in 10 min.

Solid Surfaces. Round mica stacks of 12 mm diameter were obtained from Methafix (Montdidier, France). The stacks were made opaque at the backside, to prevent double reflection, and fixed with wax over an 8 mm diameter hole in an aluminum holder. Before use, a freshly cleaved, mildly hydrophilic, mica surface was obtained by repeated removal of a few layers with Scotch tape, firmly pressed on the stack and then slowly torn off. When the removed mica layer on the tape had a regular appearance, the plate was used directly. Ellipsometric determination of the refractive index of the mica stacks showed a slight optical anisotropy, but this effect was minimized due to the fixed position of the stack in the holder.

Silicon wafers from Wacker Chemitronic (n-type, phosphorus doped) were obtained from Aurel GmbH (Landsberg, Germany) and cut into slides of 4.0 × 0.8 cm. The slides were thoroughly cleaned with detergent (Sparkleen, Calgon, Pittsburgh, PA) and water. Thereafter they were kept for 20 min at 80 °C in 30% chromic sulfuric acid (Merck, Darmstadt, Germany) and extensively rinsed with water. After such treatment, the thin silica (SiO_2) layer covering such silicon surfaces had become highly hydrophilic. Glass slides of 4.0 × 0.8 cm were cut from microscope slides (no. 02 1102; clear silica glass) obtained from Menzel-Gläser (Braunschweig, Germany). The backside was made opaque with emery paper. Before use, the slides were made highly hydrophilic by chromic acid treatment as described.

Ellipsometry. Membrane formation was measured by ellipsometry as described before.[21,22] The technique is based on reflection of light from a He−Ne laser (Spectra Physics, Mountain View, CA; $\lambda = 632.8$ nm) and measurement of the two angles ψ (psi) and Δ (delta) in the expression

$$\rho = \frac{R_p}{R_s} = \tan \psi e^{(i\Delta)} \tag{1}$$

where R_p and R_s are the total reflection coefficients for light polarized parallel and normal to the plane of incidence. The change in the angles ψ and Δ due to formation of phospholipid membranes on the reflecting surface allows measurement of phospholipid surface mass with a precision of 2−4 ng/cm^2. Measurements at room temperature were started by determination of Δ and ψ for the reflecting surface in a cuvette with 3 mL of rapidly stirred buffer. From these readings, the refractive index of the surface was determined. Then, phospholipid vesicles were added to the cuvette and new values of Δ and ψ were measured every 10−14 s.

Calculation of Layer Thickness and Refractive Index of Adsorbed Phospholipids. The thickness and refractive index of adsorbed phospholipids were calculated for an optical three-compartment system. The first medium is the buffer with refractive index n_1 and angle of incidence ϕ_1 (68°). The second medium is the phospholipid−buffer mixture adsorbed on the reflecting surface, with thickness d_2, refractive index n_2, and angle of incidence ϕ_2. The third medium is the reflecting surface with refractive index n_3 and angle of incidence ϕ_3. Values of n_1 and n_2 were taken to be real, but for n_3 a complex value was used, taking into account the possible absorption of the incident light.

The (complex) values of R_p and R_s were calculated from the relations

$$R_p = \frac{(r_{p12} + r_{r23}e^{(D)})}{(1 + r_{p12}r_{r23}e^{(D)})} \tag{2}$$

and

$$R_s = \frac{(r_{s12} + r_{s23}e^{(D)})}{(1 + r_{s12}r_{s23}e^{(D)})} \tag{3}$$

where[23]

$$D = \frac{-4\pi i d_2 n_2 \cos(\phi_2)}{\lambda} \tag{4}$$

In these expressions, $\cos(\phi_2)$ was calculated from Snell's law:

$$\cos(\phi_2) = \left[1 - \left(\frac{n_1 \sin(\phi_1)}{n_2}\right)^2\right]^{1/2} \tag{5}$$

and the Fresnel coefficients r_{p12} and r_{s12} at the 1,2-interface are given by

$$r_{p12} = \frac{(n_2 \cos(\phi_1) - n_1 \cos(\phi_2))}{(n_2 \cos(\phi_1) + n_1 \cos(\phi_2))} \tag{6}$$

and

$$r_{s12} = \frac{(n_1 \cos(\phi_1) - n_2 \cos(\phi_2))}{(n_1 \cos(\phi_1) + n_2 \cos(\phi_2))} \tag{7}$$

(18) Richter, R.; Brisson, A. *Langmuir* **2003**, *19*, 1632−1640.
(19) Beneš, M.; Billy, D.; W. Th. Hermens, W. Th.; Hof, M. 2002. Muscovite (mica) allows for the characterisation of supported bilayers by ellipsometry and confocal fluorescence correlation spectroscopy. *Biol. Chem.* **2002**, *383*, 337−341.
(20) Andree, H. A. M.; Willems, G. M.; Hauptmann, R.; Maurer-Fogy, I.; Stuart, M. C. A.; Hermens, W. Th.; Frederik, P. M.; Reutelingsperger, Ch. P. M. *Biochemistry* **1993**, *32*, 4634−4640.
(21) Cuypers, P. A.; Corsel, J. W.; Janssen, M. P.; Kop, M. M. J.; Hermens, W. Th.; Hemker, H. C. *J. Biol. Chem.* **1983**, *258*, 2426−2431.
(22) Corsel, J. W.; Willems, G. M.; Kop, J. M. M.; Cuypers, P. A.; Hermens, W. Th. *J. Colloid Interface Sci.* **1986**, *111*, 544−554.
(23) McCrackin, F. L.; Passaglia, E. R.; Stromberg, R.; Steinberg, H. L. *J. Res. Natl. Bur. Stand.* (*U.S.*) **1963**, *67A*, 363−377.

Table 1. Formation of Membranes from SUVs in Hepes Buffer

	mica				silica				glass			
	adsorption rate, ng/cm²/s	surface mass, μg/cm²	thickness, nm	refractive index	adsorption rate, ng/cm²/s	surface mass, μg/cm²	thickness, nm	refractive index	adsorption rate, ng/cm²/s	surface mass, μg/cm²	thickness, nm	refractive index
					PC + EDTA							
5 μM					0.44	0.38	9.0	1.40				
20 μM	~0.4	~0.4	~45	~1.35	1.6	>0.39	>24	<1.36	1.8	0.43	13	1.39
100 μM	~2.5	~0.9	~40	~1.38	5.8	>0.51	>80	<1.34	9.1	0.41	>24	>1.36
300 μM	~7.0	~1.1	~38	~1.38						0.40	>21	>1.36
					PC + Ca^{++}							
5 μM					0.45	0.38	10	1.39				
20 μM	1.4	0.49	21	1.38	2.3	>0.39	>24	<1.35	1.7	0.45	14	1.39
100 μM	9.9	0.55	20	1.38	6.2	>0.41	>41	<1.35	13.4	0.49	>17	<1.38
300 μM		0.61	45	1.36						0.40	>28	<1.36
					PS/PC + EDTA							
5 μM					0.52	0.36	11	1.39				
20 μM					2.2	0.39	9.5	1.40	1.6	0.42	13	1.39
100 μM	~0.07	~0.6	~10	~1.42	6.3	0.36	11	1.39	7.0	0.45	13	1.39
300 μM	~0.3	~0.6	~20	~1.37						0.46	13	1.39
					PS/PC + Ca^{++}							
5 μM					0.57	0.38	11	1.39				
20 μM	2.4	0.59	10.2	1.43	2.2	0.39	10	1.40	2.0	0.47	13	1.39
100 μM	11.7	0.66	10.1	1.45	9.5	0.38	9.9	1.40	10.0	0.54	13	1.42
300 μM		0.60	10.0	1.44						0.48	13	1.40

with similar relations for r_{p23} and r_{s23}. The value of n_3 was calculated from the relation

$$n_3 = n_1 \tan(\phi_1)\left[1 - \frac{4\rho \sin^2(\phi_1)}{(\rho + 1)^2}\right]^{1/2} \quad (8)$$

where

$$\rho = \tan(\psi)e^{(i\Delta)} \quad (9)$$

calculated from Δ and ψ as measured for the bare surface in buffer.

Values of d_2 and n_2 cannot be expressed explicitly in the measured values of Δ and ψ and the remaining optical constants of the system. Therefore, an iterative procedure was used.[23] Substitution of the expressions for R_p and R_s into the relation

$$R_p/R_s = \tan(\psi)e^{(i\Delta)} \quad (10)$$

gives a quadratic expression of the form

$$C1\,(e^{(D)})^2 + C2\,e^{(D)} + C3 = 0 \quad (11)$$

where $C1$, $C2$, and $C3$ are complex functions of the refractive indexes, angles of incidence, Δ, and ψ. For an arbitrary value of n_2, two complex values of d_2 are obtained from this expression. The true value of d_2 must however be real, and by adjustment of n_2, such as to minimize the complex part of d_2, the correct values of n_2 and d_2 were obtained.

Calculation of Adsorbed Phospholipid Surface Mass. Adsorbed phospholipid vesicles, even more so than adsorbed proteins (see below), contain water, and the adsorbed layer has a lower refractive index than pure lipids. The surface mass Γ of phospholipids in this lipid/water mixture, expressed in μg/cm², was calculated from the layer thickness d and refractive index n as described,[21] using the relation

$$\Gamma = \frac{0.3d(n - n_b)(n + n_b)}{\left[\left(\frac{A}{M}\right)(n_b^2 + 2)(n^2 + 2) - V_{20}(n_b^2 - 1)(n^2 + 2)\right]} \quad (12)$$

where d is expressed in nm, $n_b = 1.3350$ is the refractive index of the buffer solution, A and M are the molar refractivity and molecular weight of the phospholipids, and v_{20} is the specific volume of phospholipids at room temperature. The values of A/M and v_{20} used in these calculations were 0.274 and 0.890, respectively.[21]

Results

Membrane Formation on Freshly Cleaved Mica. The mean refractive index n_3 of the mica surfaces, ± standard deviation (SD), was 1.679 ± 0.022 and −0.007 ± 0.004 for the real and complex part, respectively. In the absence of calcium (2 mM EDTA), variable results were obtained, as indicated by the approximation symbol (~) in Table 1, with slow adsorption (~0.4 ng/cm²/s) for 20 μM DOPC vesicles (Figure 1) and hardly detectable adsorption of 20 μM DOPS/DOPC vesicles. Still, for sufficiently high DOPC concentrations (≥100 μM), the total phospholipid mass of adsorbed vesicles exceeded the condensed membrane mass of about 0.6 μg/cm² (see below), while for low DOPC concentrations (20 μM) adsorption remained below this value (Figure 1). From these data, the binding constant K_d of DOPC vesicles to the mica surface was estimated at about 30 μM. The high thickness of ~40 nm and low refractive index of ~1.37 of these layers indicated that they consisted of intact vesicles adhering to the surface. This is also apparent from the desorption observed after removal of the vesicles by flushing with buffer (Figure 1). The even slower adsorption of DOPS/DOPC vesicles is probably explained by electrostatic repulsion between the mica surface and the negatively charged vesicle membrane.

As also shown in Figure 1, addition of calcium of final concentration 2 mM of free Ca^{2+} ions to such DOPC layers immediately caused condensation of the adsorbed vesicles into much denser membranes, as shown by the large jumps to higher refractive index and lower thickness. For high DOPC concentrations, such fusion caused net loss of vesicles, which were apparently squeezed off during condensation. For low DOPC concentrations, condensation was followed by restart of adsorption up to full surface coverage.

As shown in the 20 μM experiment of Figure 1, however, also in the presence of calcium adsorbing DOPC vesicles did not immediately condense but retained vesicle dimensions up to about 50% of full bilayer mass. This "critical surface mass" behavior is further discussed below.

A slow further adsorption of DOPC vesicles on the condensed layers was observed, as apparent from the increasing thickness and decreasing refractive index.

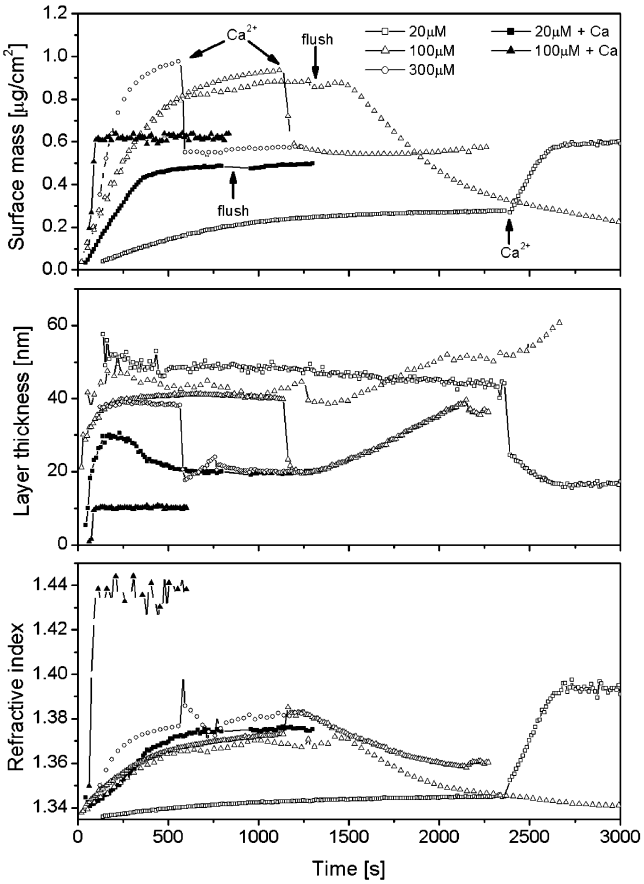

Figure 1. Time evolution of calculated surface mass, layer thickness, and refractive index after addition of different concentrations of DOPC SUVs (lipid concentrations: 20, 100, and 300 μM, respectively) to mica surfaces in the absence or presence of 2 mM calcium. "Flush" in the graph indicates flushing with respective buffer without SUVs; "Ca^{2+}" indicates adding of $CaCl_2$ to a final concentration of 2 mM.

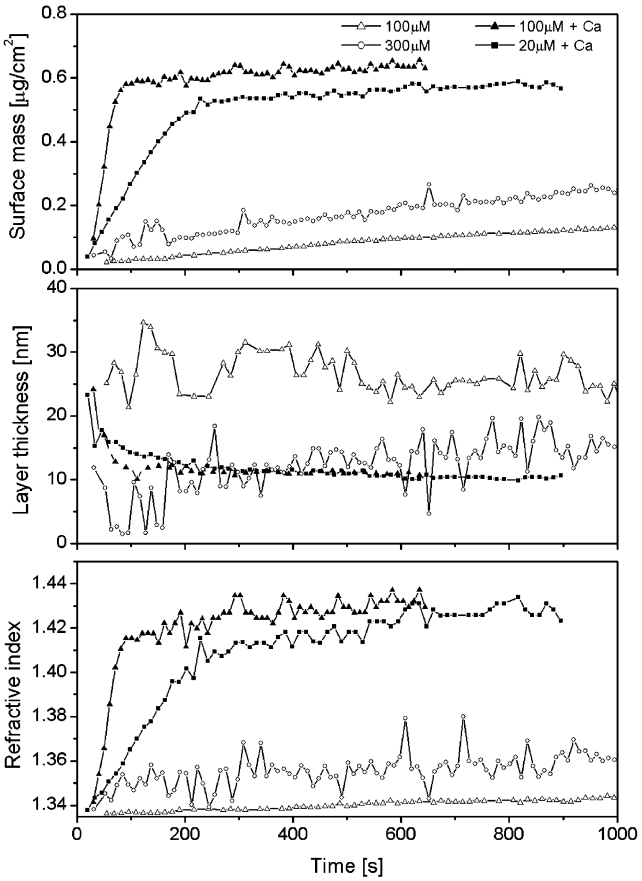

Figure 2. Time evolution of calculated surface mass, layer thickness, and refractive index after addition of different concentrations of 20%DOPS/80%DOPC SUVs (lipid concentrations: 20, 100, and 300 μM, respectively) to mica surfaces in the absence or presence of 2 mM calcium.

Membranes formed from DOPC vesicles in the presence of calcium remained stable after flushing with buffer (see Figure 1).

Similar effects of calcium are shown in Figure 2 for DOPS/DOPC vesicles. Without calcium, thick layers with low refractive indexes formed slowly, whereas condensed layers with a thickness of about 10 nm, a refractive index of about 1.42, and a final surface mass of about 0.6 μg/cm^2 were formed rapidly in the presence of 2 mM $CaCl_2$ (see Table 1). In contrast to DOPC vesicles, however, DOPS/DOPC vesicles showed no further adsorption on these membranes.

Membranes were less stable in Tris buffer than in Hepes buffer. In the presence of calcium, membranes of DOPC and DOPS/DOPC vesicles were readily formed in Tris buffer but removal of the vesicles by subsequent flushing with Tris buffer without calcium caused desorption (results not shown).

Membrane Formation on Silica. Figures 3 and 4 show the adsorption on silica surfaces of DOPC and DOPS/DOPC vesicles in Hepes buffer, either in 2 mM EDTA or in 2 mM $CaCl_2$. In contrast to the situation for mica, calcium had no effects, apart from a slightly increased formation rate for DOPC vesicles (see Table 1). The mean refractive index n_3 of the silica surfaces measured in buffer was 3.892 ± 0.012 for the real part and -0.054 ± 0.007 for the complex part. The ellipsometer sample time of about 10 s caused underestimation of the measured adsorption rates for experiments with higher phospholipid concentrations than 100 μM, and these are not included in Table 1. As further discussed below, the linear adsorption curves, almost up to final surface mass, indicate prompt fusion of adsorbed vesicles.

Initially adsorbed vesicles had a thickness of 20−40 nm and a refractive index of about 1.340, only slightly higher than the refractive index of 1.335 of pure buffer. During further adsorption, these layers then condensed into thinner and denser layers with a surface mass of about 0.40 μg/cm^2, a thickness of about 10 nm, and refractive index of about 1.40, as summarized in Table 1.

Similar to mica, DOPC vesicles slowly adsorbed to the condensed layers on silica, but DOPS/DOPC vesicles did not. A similar behavior was observed for the adsorption of POPC vesicles on monolayer-covered quartz.[12] Flushing with vesicle-free buffer (see the upper panel of Figure 3) promptly terminated this adsorption and caused a slow return to earlier parameter values. For the experiments with 20 μM, these effects were hardly detectable for surface mass but still occurred for thickness and refractive index, whereas the effect no longer occurred in the 5 μM experiments. These data suggest low-affinity binding of DOPC vesicles to the condensed membrane formed on the silica surface.

An interesting "critical surface concentration" effect was observed during membrane formation by 5 and 20 μM DOPS/DOPC vesicles. For increasing surface coverage, the thickness of the layers remained approximately constant at about 25 nm, up to 50−60% of total surface coverage. Then a transition occurred with a decrease of thickness to about 9 nm and a more rapid increase of

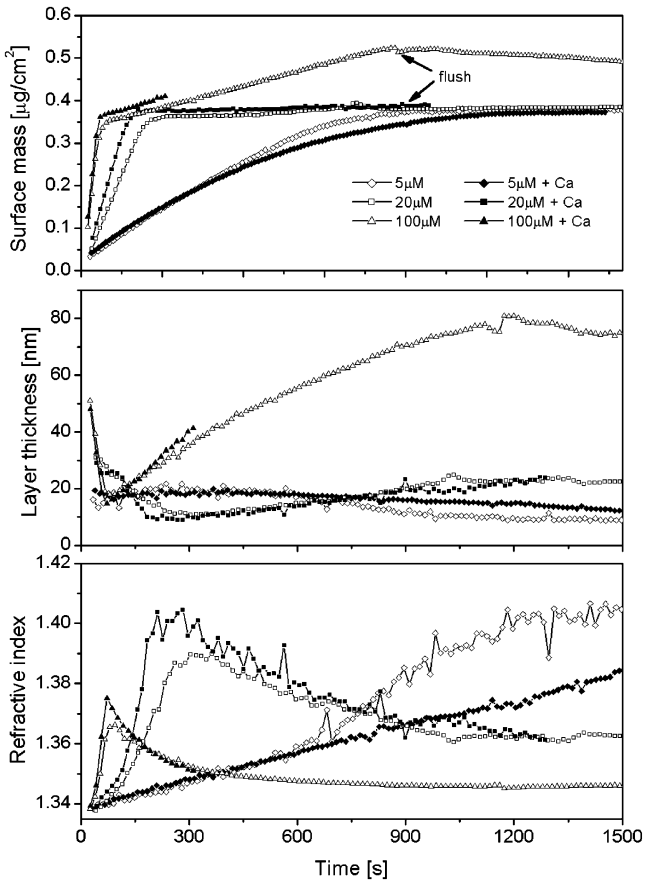

Figure 3. Time evolution of calculated surface mass, layer thickness, and refractive index after addition of different concentrations of DOPC SUVs (lipid concentrations: 5, 20, and 100 μM, respectively) to silicon surfaces in the absence or presence of 2 mM calcium. "Flush" in the graph indicates flushing with respective buffer without SUVs.

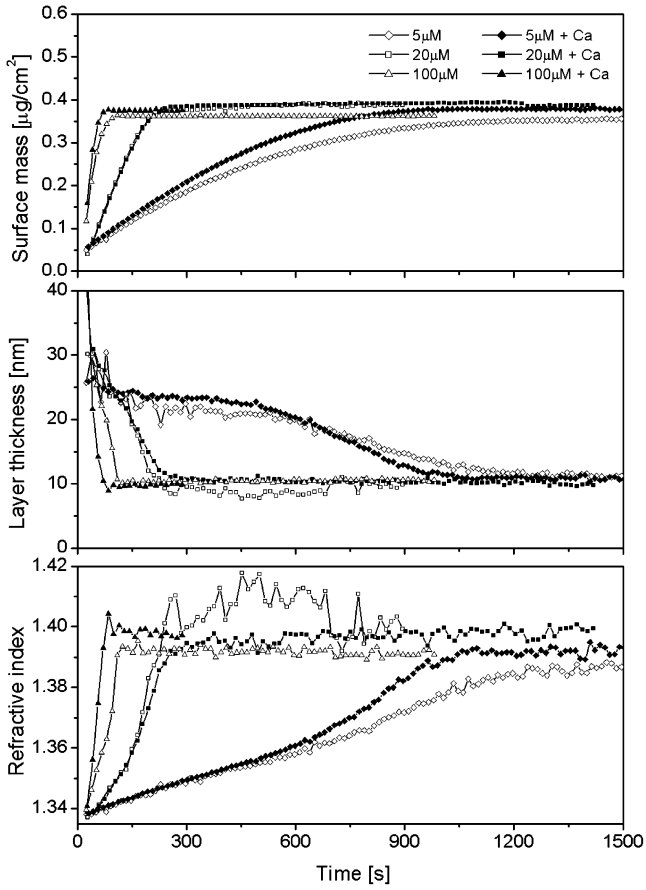

Figure 4. Time evolution of calculated surface mass, layer thickness, and refractive index after addition of different concentrations of 20%PS/80%DOPC SUVs (lipid concentrations: 5, 20, and 100 μM, respectively) to silicon surfaces in the absence or presence of 2 mM calcium.

refractive index to 1.39 (Figure 4). It seemed as if condensation of the membrane required a threshold value for the surface density of adsorbed vesicles. This threshold phenomenon was also observed for 20 μM DOPC vesicles (Figure 3).

In contrast to the situation for mica, membrane formation on silica was identical in Tris buffer and Hepes buffer.

Membrane Formation on Glass. Figure 5 presents membrane formation on hydrophilic glass slides in Hepes buffer, in the presence of either 2 mM EDTA or 2 mM $CaCl_2$. Again, identical results were obtained in Tris buffer, and only marginal effects of added calcium were found. The mean refractive index n_3 of the glass surfaces measured in buffer was 1.506 ± 0.002 (mean $\pm$ SD, $n = 12$) for the real part and -0.012 ± 0.003 for the complex part. Rapid phospholipid adsorption with adsorption rates of 1.6−2.0 ng/cm^2/s were observed, with a final surface mass of 0.40−0.54 μg/cm^2, that is, about 10% higher and more variable than on silicon slides. The average thickness was ~13 nm and the average refractive index ~1.39, except for high concentrations of DOPC vesicles. In the latter case, a similar behavior is found as for silicon slides, that is, continuing adsorption of vesicles with a large increase of thickness and a decrease of refractive index. The latter phenomenon was less prominent than for silicon slides and hardly detectable from overall surface mass, even for DOPC concentrations as high as 300 μM.

The experiment with 20 μM DOPC without calcium was repeated without stirring, and Figure 5 shows that adsorption by diffusion proceeded about 10 times slower than in the stirred system (0.15 ng/cm^2/s). Eventually, however, full membrane mass was reached (data not shown). Just like surface mass, layer thickness and refractive index eventually (after more than 1 h) reached similar values as found with stirring.

Degradation of DOPC Membranes on Mica by PLA2. Degradation of DOPC membranes by PLA2 is shown in Figure 6. All experiments were performed in Hepes buffer with 2 mM $CaCl_2$, because the hydrolytic activity of PLA2 is calcium-dependent. Membranes on mica were formed by addition of 20 μM DOPC in Hepes buffer with 2 mM calcium. Then excess vesicles were removed by flushing with Hepes buffer with calcium. Finally, 100 ng/mL of PLA2 was added at zero time. As shown in Figure 6, it took about 150 s before steady-state membrane degradation rates were established. As described earlier,[24] the desorption is transport-limited and determined by the critical micelle concentrations of degradation products in the membrane. Figure 6 also shows that the experiments with the highest and lowest values for the thickness corresponded respectively to the lowest and highest values for the refractive index, which illustrates covariant experimental scatter as further discussed below.

Discussion

In studies of the kinetics of membrane formation on solid supports, ellipsometry allows the measurement of

(24) Speijer, H.; Giesen, P. L. A.; Zwaal, R. F. A.; Hack, C. E.; Hermens, W. Th. *Biophys. J.* **1996**, *70*, 2239−2247.

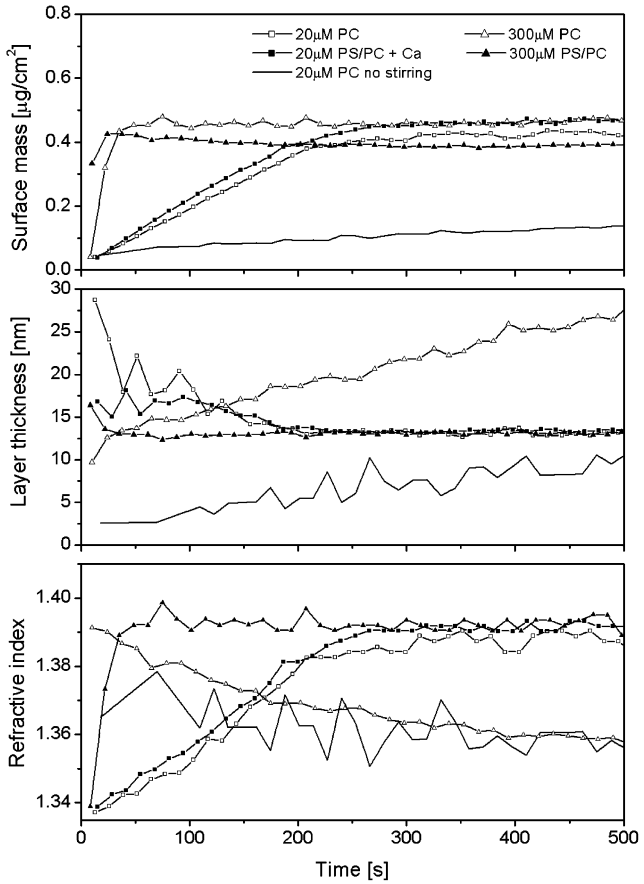

Figure 5. Time evolution of calculated surface mass, layer thickness, and refractive index after addition of different concentrations of 20%DOPS/80%DOPC or DOPC SUVs (lipid concentrations: 20 and 300 μM, respectively) to glass surfaces in the absence or presence of 2 mM calcium as well as with or without stirring.

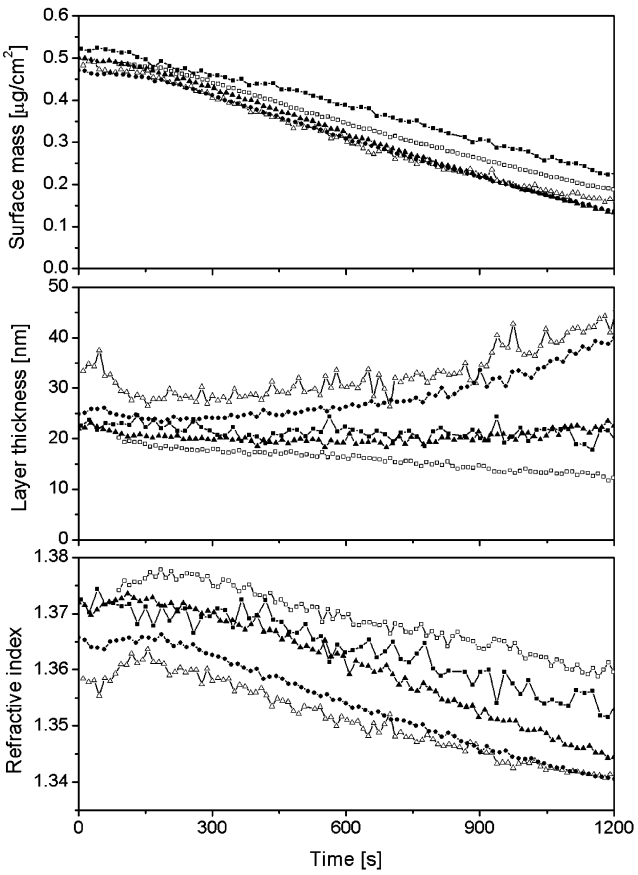

Figure 6. Time evolution of calculated surface mass, layer thickness, and refractive index during degradation of DOPC layers on mica by phospholipase A2.

rapid, simultaneous changes in relatively large surface areas. Especially for fast, cooperative, changes, for instance, the rapid condensation of adsorbed lipids into bilayers as demonstrated in the present study, this is an important advantage of ellipsometry, compared to scanning techniques with small sample areas, like AFM or scanning tunneling microscopy (STM).

The present study differs fundamentally from earlier ellipsometric studies of the formation of supported membranes that used fixed values for the refractive index n_2 of the adsorbed phospholipid layers.[25,26] Such fixed values make it impossible to detect membrane condensation. Without the corresponding increase of n_2, a decrease in thickness d_2 will not follow from the calculations. A similar limitation holds for another one-parameter technique like SPR, detecting only angle shifts. Due to the covariance of error in d_2 and n_2, ellipsometry with fixed n_2 values essentially measures only surface mass, as further explained below.

Effects of Error on the Presented Results. Figure 7 presents simulations on mica, silica, and glass. Using mean refractive index values as found for these surfaces, Δ and ψ were calculated for layers with thickness d_2 between 0 and 10 nm and refractive indices n_2 between 1.37 and 1.42. The surface mass Γ (μg/cm^2) was calculated from d_2 and n_2, and equal-mass contours are presented as dotted lines. Experimental scatter in Δ and ψ values ($\pm$0.01°) is also indicated. It follows from this figure that, for instance on mica, experimental scatter could produce values between $d_2 = 6$ nm with $n_2 = 1.42$and $d_2 = 7$ nm with $n_2 = 1.40$. As earlier demonstrated for chromium surfaces,[21] this implies covariant scatter with overestimation of d_2 causing underestimation of n_2 and vice versa (see also Figure 6). Because the expression for surface mass Γ contains the factor $d_2(n_2 - n_b)$, such covariant scatter in d_2 and n_2 implies a much smaller scatter in Γ, as illustrated in Figures 1−6 by the smoother curves for Γ.

Apart from experimental scatter, systematic error is caused by surface roughness and by imperfections of the optical components, such as nonideal polarizers and differences in light transmission along the two axes of the compensator.[23,27] For the silica and glass surfaces used in our study, surface roughness is indeed in the nanometer scale,[17] while nonideality of the compensator may introduce error dependent on the range of actually measured Δ and ψ values. It follows from Figure 7 that systematic overestimation of Δ could cause overestimation of both d_2 and n_2 and thereby, even more so, of Γ. This type of error would not invalidate the observed trends, such as calcium-induced membrane condensation, but it could affect the absolute values obtained. For instance, the measured average thickness of about 10 nm for DOPS/DOPC membranes on mica in the presence of calcium (Table 1) could be a systematic overestimation of a true thickness

(25) Puu, G.; Gustafson, I. *Biochim. Biophys. Acta* **1997**, *1327*, 149−161.

(26) Höök, F.; Vörös, J.; Rodahl, M.; Kurrat, R.; Böni, P.; Ramsden, J. J.; Textor, M.; Spencer, N. D.; Tengvall, P.; Gold, J.; Kasemo, B. *Colloids Surf., B* **2002**, *24*, 155−170.

(27) Azzam, R. M. A.; Bashara, N. M. *Ellipsometry and polarized light*; North-Holland Elsevier Science Publishers B.V.: Amsterdam, 1987.

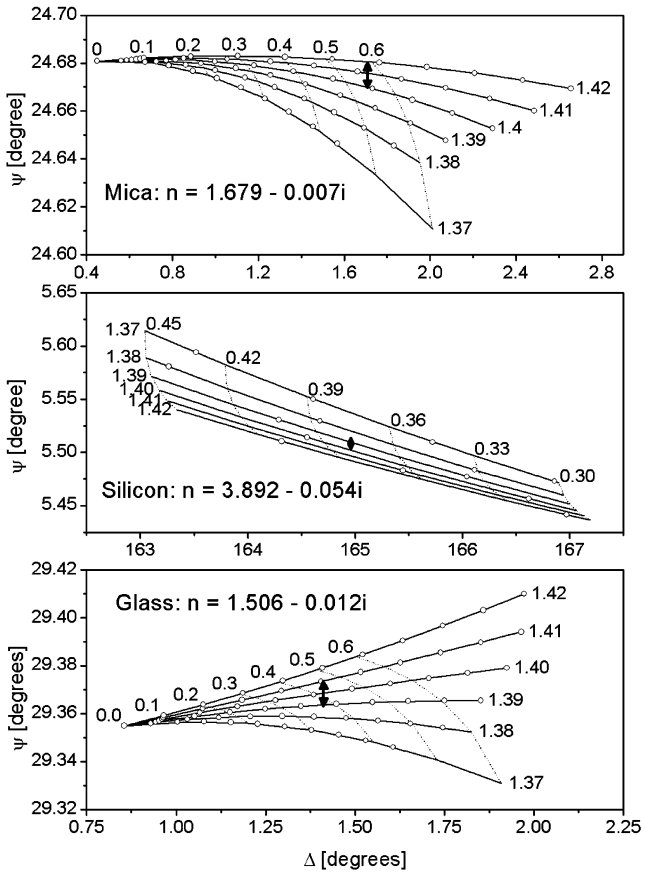

Figure 7. Simulations of measurement error on mica, silica, and glass. Plotted are calculated ellipsometry readout parameters Δ and ψ for phospholipid layers with refractive indexes ranging from 1.37 to 1.42 and with total adsorbed mass ranging from 0 to 0.6 μg/cm^2 for mica and glass surfaces and from 0.3 to 0.45 μg/cm^2 for the silicon surface.

of about 7 nm, as suggested by other methods.[3−15,28] Also, compared to the surface mass of about 0.46 μg/cm^2 on glass, the lower value of about 0.39 μg/cm^2 on silica could be caused by systematic error, dependent on the range of Δ and ψ values. Because of the similarity of Δ and ψ ranges for glass and mica, however, this could not explain the higher value of about 0.60 μg/cm^2 on mica.

Influence of Stirring and Vesicle Clustering on Adsorption Kinetics. As shown in Figure 5, stirring dramatically increases the adsorption rates, explaining why studies in unstirred systems generally use high phospholipid concentrations. For low-affinity binding, for instance, of DOPC vesicles on mica in EDTA, the adsorption rate will immediately start tapering off when free surface space diminishes. For high-affinity binding, however, the adsorption rate will be "transport-limited", that is, totally determined by stirring and diffusion, and will remain constant up to high surface coverage. This is also promoted by clustering of adsorbed vesicles.[29,30] Isolated vesicles on a surface will each exclude 4 times their own surface area from further adsorption. In a cluster, however, each vesicle will exclude only little more than its own surface area.

As shown in Figures 3 and 4, constant adsorption rates were observed for vesicle adsorption on silica, with deviations from linearity only occurring for a surface mass exceeding 90% of full surface coverage. Indeed, a study of vesicle adsorption on a rotating silicon disk, a system allowing analytical solution of the convection−diffusion equation, found transport-limited adsorption of vesicles as used in the present study on hydrophilic silica surfaces.[31]

Mechanisms of Membrane Formation on Solid Supports. On theoretical grounds, it was proposed that an increasing contact area between vesicle and support causes increasing wall stress leading to "bursting" of the vesicle, with exposure of its inner membrane.[32] Experimental studies, however, have presented evidence for a "spreading" mechanism with the vesicle opening on the surface and exposing its outside membrane.[33,34] Recently, a "sliding" mechanism was proposed,[28] by which the top bilayer of totally flattened vesicles slides from the bottom bilayer. The exposed membrane would then originate from the outside as well as the inside of the vesicle.

Vesicle−vesicle interactions were not considered in these models, but a study using QCM-D has indicated the existence of a critical surface concentration of vesicles required for membrane condensation on hydrophilic silica surfaces.[35] This concept has been confirmed in a recent fluorescence study, showing that isolated vesicles adsorbed on quartz surfaces remained intact but showed signs of rupture and fusion after adsorption of nonfluorescent vesicles.[36] In the present study, a similar phenomenon was observed for silica surfaces and low (5 and 20 μM) vesicle concentrations. For high concentrations, this phenomenon was below our time resolution.

Calcium-induced membrane condensation was found on mica for DOPS/DOPC vesicles, which have a strong electrostatic interaction with calcium, but also for pure DOPC vesicles, which are electrically neutral at physiological pH and have no, or only weak, affinity for calcium. The fact that calcium still induced condensation of the latter vesicles suggests that direct vesicle−vesicle interactions are not the driving force of the condensation process. Apparently, calcium modifies the mica surface, for instance, by binding to it, and this modification changes vesicle−surface interactions and initiates the condensation process. These findings plead against an important role of calcium bridges between the negatively charged mica surface and negatively charged (parts of the) biomolecules.[37] Apparently calcium modifies the mica surface in a way that also promotes adsorption of vesicles from uncharged DOPC.

It has been claimed that freshly cleaved mica in contact with water will be covered by a structured, "icelike", water layer.[38] Such a layer could prevent the intimate contact needed for vesicle spreading on the surface. Direct interaction of calcium with the mica surface could then expel the water layer and thus trigger membrane formation. The instability of membranes on mica in Tris buffer could be related to Tris-induced rippled phospholipid

(28) Jass, J.; Tjärnhage, T.; Puu, G. *Biophys. J.* **2000**, *79*, 3153−3163.
(29) Willems, G. M.; Hermens, W. Th.; Hemker, H. C. *J. Biomater. Sci., Polym. Ed.* **1991**, *2*, 217−226.
(30) Zhdanov, V. P.; Keller, C. A.; Glasmästar, K.; Kasemo, B. *J. Chem. Phys.* **2000**, *112*, 900−909.
(31) Giesen, P. L. A.; Hemker, H. C.; Hermens, W. Th. *Biochim. Biophys. Acta* **1995**, *1237*, 43−48.
(32) Seifert, U. *Adv. Phys.* **1997**, *46*, 13−137.
(33) Contino, P. B.; Hasselbacher, C. A.; Ross, J. B. A.; Nemerson, Y. *Biophys. J.* **1994**, *67*, 1113−1116.
(34) Salafsky J.; Groves, J. T.; Boxer, S. G. *Biochemistry* **1996**, *35*, 14773−14781.
(35) Keller, C. A.; Glasmästar, K.; Zhdanov, V. P.; Kasemo, B. *Phys. Rev. Lett.* **2000**, *84*, 5443−5446.
(36) Johnson, J. M.; Chu, T.; Ha, S.; Boxer, S. G. *Biophys. J.* **2002**, *83*, 3371−3379.
(37) Kawanishi, N.; Christenson, H. K.; Ninham, B. W. *J. Phys. Chem.* **1990**, *94*, 4611−4617.
(38) Cantrell, W.; Ewing, G. E. *J. Phys. Chem.* **2001**, *B105*, 5434−5439.

Table 2. Data from the Literature on Supported Membranes[a]

reference	support (polarity)	lipids (mole ratio)	lipid preparation	buffer (mM NaCl/mM Ca) with additives	observation method	membrane structure
Brian, 1984	glass (+)	egg PC/Chol (7/2)	DUVs	10 mM Tris (140/0)	TIRF/FRAP	fused
	glass (−)	with protein				fused
Bayerl, 1990	glass (+)	DMPC	SUVs water		^{2}H NMR	bilayers
Kalb, 1992	quartz (+)	POPG/POPC (1/4) or POPC	EUVs	10 mM Tris (150/0)	TIRF/FRAP	fused
	quartz (−)					fused/ves
Nollert, 1995	glass (+)	POPC	EUVs	10 mM Hepes (0/0)	fluorescence	bilayers
		E. coli lipid		with 40 mM Na_2SO_4	energy transf and FRAP	vesicles
		E. coli lipid		with 20 mM Ca^{++}		bilayers
Giesen, 1995	silica (+)	DOPS/DOPC (2/3)	SUVs	50 mM Tris (100/3)	ellipsometry and catalysis	bilayers
Puu, 1997	silica (+)	DPPC/DPPG/DPPE/Chol (50/20/22.5/7.5)	DUVs	20 mM Tris (100/0)	ellipsometry and SPR	no adsorption
		DOPC		±20 mM Ca^{++}		vesicles (rev)
Keller, 1998	silica (+)	egg PC	SUVs	10 mM Tris (100/0)	QCM-D	bilayers
	gold (+)					vesicles
Reviakine, 2000	silica (+)	egg PC or DOPC	SUVs	10 mM Hepes (40/0)	AFM	bilayers
	mica (+/−)					vesicles
	mica (+/−)	egg PC or DOPC		10 mM Hepes (150/2)		bilayers
	mica (+/−)	DOPS/DOPC		with 3 mM NaN_3		bilayers
Jass, 2000	silica (+)	DPPC/DPPE/DPPG/Chol (8/5/4/1) + 10% glycolipid	DUVs	20 mM Tris (100/0) with 0.02% Na_2SO_4	AFM	bilayers
Reimhult, 2002	silica (+)	egg PC	SUVs/	10 mM Tris (100/0)	QCM-D	bilayers
	TiO_2 (+)		DUVs			vesicles
present study	mica (+/−)	DOPC	SUVs	10 mM Hepes (150/0)	ellipsometry	vesicles (rev)
		DOPC		10 mM Hepes (150/2)		bilayers + ves
		DOPS/DOPC (1/4)		10 mM Hepes (150/0)		vesicles
		DOPS/DOPC (1/4)		10 mM Hepes (150/2)		bilayers
	silica (+)	DOPC		10 mM Hepes (150/0)		bilayers + ves
		DOPC		10 mM Hepes (150/2)		bilayers + ves
		DOPS/DOPC (1/4)		10 mM Hepes (150/0)		bilayers
		DOPS/DOPC (1/4)		10 mM Hepes (150/2)		bilayers
	glass (+)	DOPC		10 mM Hepes (150/0)		bilayers + ves
		DOPC		10 mM Hepes (150/2)		bilayers
		DOPS/DOPC (1/4)		10 mM Hepes (150/0)		bilayers
		DOPS/DOPC (1/4)		10 mM Hepes (150/2)		bilayers

[a] Abbreviations: PC, phosphatidylcholine; PG, phosphatidylglycerol; PS, phosphatidylserine; PE, phosphatidylethanolamine; DMPC, dimyristoyl-PC; DPPC, dipalmitoyl-PC; DOPC, dioleoyl-PC; POPC, palmitoyl-oleoyl-PC; DOPS, dioleoyl-phosphatidylserine; Chol, cholesterol; SUV, sonicated unilamellar vesicles (15−30 nm diameter); EUV, extruded unilamellar vesicles (30−200 nm diameter); DUV, detergent-depleted unilamellar vesicles (200−400 nm diameter); AFM, atomic force microscopy; ^{2}H NMR, deuterium nuclear magnetic resonance; TIRF, total internal reflection fluorescence; FRAP, fluorescence recovery after photobleaching; SPR, surface plasmon resonance; QCM-D, quartz crystal microbalance-dissipation.

phases observed in supported bilayers on mica.[39] On silica and glass, no differences were found between the results in Hepes and Tris, once again indicating the dominant role of surface properties on membrane formation.

Degradation of Phospholipid Membranes by PLA2. The hydrolysis of supported phospholipid membranes by PLA2 has recently been studied by AFM.[8,40] In these studies, bilayers of phospholipids in the gel phase (dipalmitoyl-phosphatidylcholine, DPPC) were deposited on freshly cleaved mica by the classical Langmuir−Blodgett stacking technique. It was found that the action of PLA2 started at the edges of local defects in such membranes, caused by mechanical stress during stacking, and for some time remained proportional to the increasing length of these edges due to the breakdown of phospholipids by PLA2. After some time, the membrane consisted of intact patches of phospholipids, separated by increasing gaps from which the phospholipids had disappeared.

These results are only partly supported by the present study. The DOPC mixture was in the fluid phase, and gaps in the membrane will be filled due to rearrangement and additional vesicle adsorption, producing DOPC membranes on mica without significant defects.[3−15] So the present study indicates that fully intact membranes can also be attacked by PLA2. However, as also shown in Figure 6, the thickness of DOPC layers remained essentially unaltered during degradation, and the refraction index showed a steady decline from about 1.367 to 1.350. This behavior is consistent with a gradual decrease of membrane density (refractive index), with a stable thickness of the remaining patches of phospholipid.[8,40] Apparently, even for only partial surface coverage, obtained values of membrane thickness and refractive index can be correctly interpreted.

Data from the Literature. Table 2 presents data from the literature relevant to the present study. The polarity (wettability) of the surfaces, as influenced by cleaning procedures or by special treatments such as alkylation or thiolation, is indicated. Membranes were formed by exposure of the support to unilamellar vesicles in buffer or water with pH values between 7.4 and 8.0. Unilamellar vesicles were obtained by sonification (SUVs), extrusion through filters (EUVs), or detergent depletion (DUVs).

Supported membrane preparations were classified as "vesicles", "fused", or "bilayers", or their combination like the initial formation of a bilayer with subsequent adherence of vesicles. Fusion was assumed to have occurred when a normal lateral lipid/protein mobility was demonstrated, in most cases with FRAP (fluorescence recovery after photobleaching). As explained, linear adsorption kinetics is also highly suggestive of fusion. A fused membrane was considered a bilayer when surface mass equaled bilayer mass. For AFM, a defect-free layer of bilayer thickness was assumed to demonstrate a bilayer. Because of experimental error and unknown factors such as surface roughness, the presence of a water layer between membrane and support, or packing with tilted

(39) Mou, J.; Yang, J.; Shao, Z. *Biochemistry* **1994**, *33*, 4439−4443.
(40) Nielsen, L. K.; Risbo, J.; Callisen, T. H.; Bjørnholm, T. *Biochim. Biophys. Acta* **1999**, *1420*, 266−271.

hydrocarbon chains, a rough agreement was accepted in these definitions.

Conclusions. The present study indicates that bilayer formation of adsorbed vesicles is strongly dependent on the adsorbing surface. For glass, direct vesicle−surface interaction seems to dominate and adsorbed vesicles immediately form bilayers, irrespective of phospholipid composition or the presence of calcium. Therefore, the rate of bilayer formation is only dependent on the rate of vesicle adsorption, that is, on vesicle concentration in the buffer and flow conditions. Vesicle−vesicle interactions were only apparent from some additional adsorption of DOPC vesicles to the bilayer.

For silica, the situation was more complicated. Phospholipid composition again had little influence on vesicle adsorption, but calcium had a slightly accelerating effect. More important, bilayer formation was dependent on the surface concentration of vesicles and required a critical surface mass of about 50% of full bilayer mass. Apparently, vesicle−surface as well as vesicle−vesicle interactions were important in bilayer formation. Reversible adsorption of DOPC vesicles to preformed bilayers was more apparent than for glass, indicating some influence of the surface on bilayer properties.

For mica, the presence of calcium was a dominant factor and phospholipid composition also played a role. In the absence of calcium, the mica surface had limited affinity for vesicle adsorption. DOPC vesicles adsorbed slowly and reversibly, while retaining their vesicle structure, and negatively charged DOPS/DOPC vesicles adsorbed even slower, probably because of electrostatic repulsion by the mica surface. Addition of calcium caused higher vesicle adsorption rates and, for already adsorbed vesicles, prompted condensation into bilayers. Again, however, the condensation process seemed to require a surface mass of more than about 50% of bilayer mass.

Table 2 confirms the major role of surface properties in bilayer formation. Vesicle preparations that readily formed bilayers on hydrophilic silica surfaces produced layers of nonfused adhering vesicles on oxygen-treated hydrophilic gold or TiO_2 surfaces.[14,41] The major role of calcium for results on mica is also confirmed.[3−15] For multicomponent mixtures, which usually adsorb less readily than pure lipids or binary mixtures, phospholipid composition may also be important. Addition of 10% glycolipid (galactocerebroside, type II) to a mixture of DPPC, dipalmitoylphosphatidylethanolamine, dipalmitoyl-phosphatidylglycerol, and cholesterol produced bilayers on silica.[28]

Acknowledgment. A large part of this work was performed with support from the European Union through Marie Curie Ph.D. fellowships of M. Beneš and A. Benda in Maastricht (QLK5-CT-2000-60007, 1 and 10). We also thank Professor A. Brisson and Dr. R. Richter, from the Institut Européen de Chimie et Biologie, Bordeaux, France, for stimulating discussions and suggestions and for providing mica stacks. The financial support of the Ministry of Education, Youth and Sports of the Czech Republic (via LN 00A032) and the Dutch Heart Foundation (Grant 97.147) is also gratefully acknowledged.

LA048811U

(41) Reimhult, E.; Höök, F.; Kasemo, B. *J. Chem. Phys.* **2002**, *117*, 7401−7404.